Molecular and Cellular Pathobiology

Cancer Research

Oncogenic *BRAF* Mutation with *CDKN2A* Inactivation Is Characteristic of a Subset of Pediatric Malignant Astrocytomas

Joshua D. Schiffman[1], J. Graeme Hodgson[2], Scott R. VandenBerg[4], Patrick Flaherty[5], Mei-Yin C. Polley[2], Mamie Yu[2], Paul G. Fisher[6], David H. Rowitch[2,3], James M. Ford[7], Mitchel S. Berger[2], Hanlee Ji[7], David H. Gutmann[8], and C. David James[2]

Abstract

Malignant astrocytomas are a deadly solid tumor in children. Limited understanding of their underlying genetic basis has contributed to modest progress in developing more effective therapies. In an effort to identify such alterations, we performed a genome-wide search for DNA copy number aberrations (CNA) in a panel of 33 tumors encompassing grade 1 through grade 4 tumors. Genomic amplifications of 10-fold or greater were restricted to grade 3 and 4 astrocytomas and included the *MDM4* (1q32), *PDGFRA* (4q12), *MET* (7q21), *CMYC* (8q24), *PVT1* (8q24), *WNT5B* (12p13), and *IGF1R* (15q26) genes. Homozygous deletions of *CDKN2A* (9p21), *PTEN* (10q26), and TP53 (17p3.1) were evident among grade 2 to 4 tumors. BRAF gene rearrangements that were indicated in three tumors prompted the discovery of KIAA1549-BRAF fusion transcripts expressed in 10 of 10 grade 1 astrocytomas and in none of the grade 2 to 4 tumors. In contrast, an oncogenic missense BRAF mutation ($BRAF^{V600E}$) was detected in 7 of 31 grade 2 to 4 tumors but in none of the grade 1 tumors. $BRAF^{V600E}$ mutation seems to define a subset of malignant astrocytomas in children, in which there is frequent concomitant homozygous deletion of CDKN2A (five of seven cases). Taken together, these findings highlight BRAF as a frequent mutation target in pediatric astrocytomas, with distinct types of BRAF alteration occurring in grade 1 versus grade 2 to 4 tumors. *Cancer Res; 70(2); 512–9. ©2010 AACR.*

Introduction

Targeted molecular therapeutics holds great promise for the development of less toxic and more effective personalized treatment strategies for cancer (1). This approach, however, requires a detailed understanding of the molecular alterations that drive tumor formation and malignant progression. The identification of seminal changes in cancer can be used to inform the development of therapeutic agents that specifically inhibit the gene products and pathways that are deregulated in association with these changes. This strategy has been used successfully in adult high-grade astrocytomas, leading to clinical trials that target the epidermal growth factor receptor (EGFR), for example. However, astrocytomas in children are distinct clinical entities from those seen in adults and do not harbor many of the critical genetic alterations found in their adult counterparts (2–5). It is therefore important that the molecular alterations unique to pediatric astrocytomas are identified and characterized.

Recently, it was shown that the majority of pilocytic astrocytomas (PA; WHO grade 1) harbor 7q34 duplications (6), which result in gene fusions between *KIAA1549* and *BRAF* (7), and concomitant expression of *KIAA1549:BRAF* fusion transcripts (7–9). Although this discovery suggests that targeted inhibition of BRAF or relevant downstream signaling mediators may be especially effective for the treatment of PA, identification of therapeutically informative molecular alterations in pediatric malignant astrocytomas (WHO grades 2, 3, and 4) has been an elusive goal.

To provide a more detailed characterization of the spectrum of genetic alterations in all malignancy grades of pediatric astrocytoma, we report a genome-wide analysis of DNA copy number alterations for a series of these tumors, presented in combination with the sequence analysis of five relevant genes, including three frequently mutated in adult astrocytomas (*TP53, PTEN*, and *IDH1*) and two involved in

Authors' Affiliations: [1]Divison of Pediatric Hematology/Oncology and Department of Oncological Sciences, University of Utah, Salt Lake City, Utah; [2]Department of Neurological Surgery, University of California at San Francisco; [3]Department of Pediatrics, Howard Hughes Medical Institute and Eli and Edythe Broad Institute for Regeneration Medicine and Stem Cell Research, San Francisco, California; [4]Department of Pathology, University of California at San Diego, La Jolla, California; Departments of [5]Biochemistry and Cancer Biology Program, [6]Neurology, and [7]Medical Oncology, Stanford University, Palo Alto, California; and [8]Department of Neurology, Washington University School of Medicine, St. Louis, Missouri

Note: Supplementary data for this article are available at Cancer Research Online (http://cancerres.aacrjournals.org/).

Current address for J.G. Hodgson: Division of Oncology, Pfizer Laboratories, La Jolla, California.

Corresponding Author: C. David James, Department of Neurological Surgery, University of California at San Francisco, 1450 3rd Street, San Francisco, CA 94143-0520. Phone: 415-476-5876; Fax: 415-514-9792; E-mail: david.james@ucsf.edu.

doi: 10.1158/0008-5472.CAN-09-1851

mitogen-activated protein kinase (MAPK) signaling (*BRAF* and *KRAS*). Our results confirm that genes targeted for sequence alteration in adult astrocytomas are less frequent mutation targets in pediatric astrocytomas. In addition, we show that *BRAF* fusion is a signature event in PA, but not in the malignant astrocytomas, whereas *BRAF* activating mutation is common in grade 2 to 4 tumors. Moreover, we found that the majority of grade 2 to 4 tumors with *BRAF* activating mutation have concomitant *CDKN2A* homozygous deletion (HD). Collectively, these findings suggest that the combination of *BRAF* activation and *CDKN2A* inactivation may be unique drivers of malignancy in a subset of pediatric astrocytomas, and whose alteration suggest targets for future therapeutic drug design.

Materials and Methods

Clinical specimens. A total of 41 astrocytomas were included in this study. Nonneoplastic brain samples derived from epileptic surgeries from pediatric (n = 2) and adult (n = 6) patients were also included. All samples were subjected to detailed histopathologic review (S.R.V.) and approved for use according to Committee on Human Research guidelines. Sufficient RNA was obtained from all cases for determination of presence or absence of *KIAA1549-BRAF* fusion transcripts, and sufficient DNA was obtained from 40 cases for gene sequence analysis. DNA from 33 of the cases was examined for copy number alterations.

Identification of copy number aberrations. To identify copy number gains and losses, we used the custom-designed molecular inversion probe (MIP) cancer panel consisting of 24,037 single-nucleotide polymorphisms (SNP; Affymetrix). The MIP assay and analysis of resultant data were performed as described (10, 11) using 37 ng of genomic DNA as starting material. The fraction of the genome altered (FGA) for each tumor was calculated as the total length of gained and deleted loci divided by the total genome length (2,866 Mb; National Center for Biotechnology Information Build 35).

Assessment of* KIAA1549-BRAF *fusion transcripts. Total RNA was extracted using the miR-Vana RNA isolation kit (Applied Biosystems), and first-strand cDNA was generated using the High Capacity cDNA Reverse Transcription kit (Applied Biosystems). PCR was conducted using 60 ng cDNA and final concentrations of 2.5 mmol/L $MgCl_2$, 25 nmol/L deoxynucleotide triphosphates (dNTP), 400 nmol/L primers, and 0.05 unit/μL AmpliTaq Gold (Applied Biosystems). Cycling conditions were as follows: 95°C for 10 min, 35 cycles of 95°C for 15 s, 55°C for 30 s, 72°C for 1 min, followed by 72°C for 10 min and 4°C hold. The forward primer, 5′-CGGAAACACCAGGTCAACGG-3′ (*KIAA1549* exon 15), and reverse primer, 5′-GTTCCAAATGATCCAGATCCAATTC-3′ (*BRAF* exon 11), used in this study detect three fusion transcripts: *KIAA1549*-exon-15/*BRAF*-exon-9, *KIAA1549*-exon-16/*BRAF*-exon-11, and *KIAA1549*-exon-16/*BRAF*-exon-9 (7). Wild-type *BRAF* primers were as follows: forward, 5′-TTGTGACTTTTGTCGAAAGCTGC-3′, and reverse, 5′-AAGGGGATGATCCAGATGTTAGG-3′.

Gene sequence analysis. For $BRAF^{V600E}$ mutation analysis, genomic DNA was PCR amplified using *BRAF* exon 15 primers with M13 tails: forward, 5′-TGTAAAACGACGGCCAGTCATAATGCTTGCTCTGATAGGA-3′; reverse, 5′-AGCGGATAACAATTTCACACAGGCCAAAAATTTAATCAGTGGA-3′. PCR final concentrations (25 μL volume) were 2.0 mmol/L $MgCl_2$, 250 nmol/L dNTPs, 0.02 unit/μL AmpliTaq Gold, 0.2 mg/mL bovine serum albumin, 500 nmol/L primers, and 10 ng of genomic DNA. Cycling conditions were as follows: 95°C for 10 min, 35 cycles at 95°C for 15 s, 64°C for 45 s, 72°C for 1 min, followed by 72°C for 10 min and 4°C hold. PCR products were treated with ExoSAP (USB) per the manufacturer's protocol and sequenced (ELIM Biopharmaceuticals).

For analysis of *IDH1* sequence alterations, we used the protocol described by Balss and colleagues (12). Briefly, a fragment of 129-bp length spanning the catalytic domain of *IDH1*, including codon 132, was amplified using the sense primer IDH1f (5′-CGGTCTTCAGAGAAGCCATT-3′) and the antisense primer IDH1r (5′-GCAAAATCACATTATTGCCAAC-3′). PCR conditions, using 20 ng DNA, were for 35 cycles with denaturing at 95°C for 30 s, annealing at 56°C for 40 s, and extension at 72°C for 50 s. Sequencing was with sense primer IDH1f (5′-CGGTCTTCAGAGAAGCCATT-3′).

KRAS mutations were identified as described by Lièvre and colleagues (13). Specific probes for mutated and nonmutated alleles labeled with fluorescence reporter dyes were included in 5 μL of reaction mixtures containing 10 ng DNA, 1 μg of specific primers and probes, and 1 μL of Taqman Universal PCR Master Mix (Applied Biosystems). Reaction mixtures were subjected to the following cycle conditions: 95°C for 15 min; 40 cycles, 95°C for 15 s; and 60°C for 1 min. The single mutation detected by allelic discrimination was confirmed by direct sequencing of exon 2 of the *KRAS* gene.

Phospho-MAPK immunohistochemistry. All tissue was routinely fixed in either phosphate-buffered 4% formalin, dehydrated by graded ethanols, and embedded in wax (Paraplast Plus, McCormick Scientific) using routine techniques. Immunohistochemistry was performed using the Benchmark XT (Ventana Medical Systems) and the Ultraview (multimer) detection system. All sections were cut at 5 μm and mounted on SuperFrost/Plus slides (Fisher Scientific). Epitope retrieval was performed for 30 min in Tris buffer (pH 8) at 90°C before application of the primary antibodies. Rabbit polyclonal antibodies to phospho-MAPK (pMAPK; extracellular signal-regulated kinase 1/2; Invitrogen) were used at a dilution of 1:200 with an incubation time of 2 h at 37°C.

Results

To identify regions of genomic copy number gain and loss, we analyzed DNA from 33 astrocytomas (Table 1) using a panel of ~24,000 MIPs enriched for sequences that directly interrogate allele-specific copy number of ~1,000 known cancer genes. Included in this analysis were 2 grade 1 tumors, 11 grade 2 tumors, 9 grade 3 tumors, and 11 grade 4 tumors. Calculation of the mean FGA for each grade of tumor revealed increasing FGA with increasing malignancy grade (grade 1 < 0.000; grade 2 = 0.016; grade 3 = 1.375; grade 4 = 2.964), with

Table 1. Summary of pediatric astrocytoma gene and genomic alterations

	Tumor	Class	Age	Location	FGA	BRAF	Other
1	SF2085	PA (I)	8	Cerebellum	ND	K16-B9	None
2	SF2415	PA (I)	9	Cerebellum	ND	K16-B9	None
3	SF2420	PA (I)	9	Brain stem	0.000	K15-B9	None
4	SF2974	PA (I)	4	Cerebellum	ND	K16-B11	None
5	SF3526	PA (I)	5	Cerebellum	ND	K16-B9	ND
6	SF3663	PA (I)	14	Optic nerve	ND	K15-B9	None
7	SF3975	PA (I)	2	Temporal	ND	K15-B9	None
8	SF4035	PA (I)	12	Spinal cord	ND	K16-B9	None
9	SF4282	PA (I)	1	Posterior fossa	0.000	K16-B9	None
10	SF4283	PA (I)	5	Cerebellum	ND	K15-B9	None
11	SF2652	DLGA (II)	10	Hypothalamus	0.014	N	None
12	SF2995	DLGA (II)	17	Unspecified	0.000	ND	ND
13	SF3094	DLGA (II)	15	Temporal	0.010	N	None
14	SF3310	DLGA (II)	17	Intraventricular	0.000	N	None
15	SF4762	DLGA (II)	21	Unspecified	0.001	N	None
16	SF4825	DLGA (II)	10	Parietal	0.000	N	None
17	WU12516	DLGA (II)	19	Brain stem	0.096	V600E	CDKN2A (HD)
18	WU12517	DLGA (II)	20	Occipital lobe	0.056	V600E	CDKN2A (HD)
19	WU108305	DLGA (II)	13	Thalamus/pineal	0.000	N	None
20	WU108309	DLGA (II)	3	Cerebellar vermis	0.000	N	None
21	WU108312	DLGA (II)	1	Frontal	0.001	N	None
22	SF1692	AA (III)	<1	Frontal	0.003	N	None
23	SF1734	AA (III)	13	Temporal	0.025	V600E	None
24	SF1752	AA (III)	5	Frontal	0.000	V600E	CDKN2A (HD)
25	SF1762	AA (III)	14	Intraventricular	1.158	N	TP53, 273:R>H
26	SF2007)*	AA (III)	13	Cerebellum	0.131	V600E	None
27	SF2390	AA (III)	11	Temporal	7.198	N	CDKN2A (HD) CCND2/WNT5B (A)
28	SF2570	AA (III)	15	Brain stem	3.860	N	TP53, 272:V>L
29	SF7269	AA (III)	7	Thalamus	0.000	N	None
30	SF7432	AA (III)	11	Brain stem	0.000	N	None
31	SF1983	GBM (IV)	9	Posterior fossa	5.137	N	TP53, 179:H>Y
32	SF2975	GBM (IV)	7	Frontal	8.001	N	CDKN2A (HD) PTEN (HD) TP53 (HD)
33	SF3343	GBM (IV)	2	Basal ganglia	0.001	N	None
34	SF4212	GBM (IV)	14	Parietal	0.984	N	KRAS: 12 G>V
35	SF4532	GBM (IV)	17	Parietal	0.722	V600E	CDKN2A (HD)
36	SF4635	GBM (IV)	17	Parietal	0.262	V600E	CDKN2A (HD)
37	SF4761	GBM (IV)	17	Parietal	5.562	N	TP53, 273:R>H PDGFRA/KIT (A)
38	SF4870	GBM (IV)	6	Parietal	4.296	N	PDGFRA/KIT (A) MET (A) IGFR1 (A)
39	SF6751	GBM (IV)	13	Parietal	4.113	N	None
40	SF6906	GBM (IV)	16	Parietal	1.736	N	PTEN: 214 T>STOP CHIC2 (A)
41	SF7124	GBM (IV)	9	Temporal	3.790	N	TP53, 172:V>F PIK3C2B/MDM4 (A) MYC/PVT1 (A)

NOTE: Missense mutations resulting in amino acid changes are indicated by amino acid sequence number and resulting amino acid change. No IDH1 mutation was identified in this tumor series.

Abbreviations: DLGA, diffuse infiltrating low-grade astrocytoma; AA, anaplastic astrocytoma; GBM, glioblastoma; A, high-level amplification.

*Recurrent tumor initially diagnosed as grade III astrocytoma.

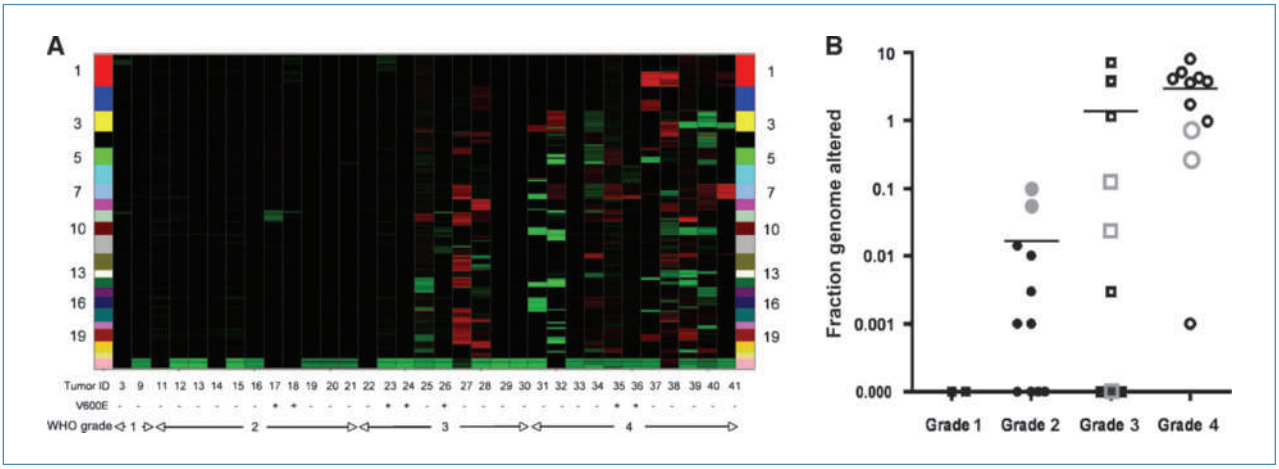

Figure 1. Copy number changes in pediatric astrocytoma. *A*, heat map showing genome-wide copy number gains (*red*) and losses (*green*) in 33 pediatric astrocytomas. Individual astrocytomas are arranged left to right on the *X* axis from low to high grade. Tumors with (+) and without (–) $BRAF^{V600E}$ mutations are indicated. Chromosome landmarks are listed vertically on both sides of the map. Note the minor number of red and green blocks among grade 1 and 2 tumors. *B*, vertical scatter plot showing individual and mean FGA values for each malignancy grade of tumor. Gray colored data points represent cases with $BRAF^{V600E}$ mutations.

the mean FGA for combined grade 3 + grade 4 tumors significantly higher than for grade 1 + grade 2 tumors ($P < 0.003$, two-sided Wilcoxon rank-sum test; Table 1; Fig. 1).

Several locations of copy number alteration were observed among grade 2 to 4 tumors. Among these, high-level amplifications (>10 copies) were observed exclusively in grade 3 and 4 tumors and included known oncogenes *MDM4* (1q32), *PDGFRA* (4q12), *MET* (7q21), *CMYC* (8q24), *PVT1* (8q24), *WNT5B* (12p13), and *IGF1R* (15q26; Fig. 2*A*). In contrast to adult grade 3 and 4 astrocytomas, no high-level or focal copy number gains for *EGFR* were observed. Regions of HD (less than one copy) were observed in grade 2 to 4 astrocytomas, involving *CDKN2A* (seven tumors; Fig. 2*B*), *PTEN* (one tumor), and *TP53* (one tumor; Table 2; Supplementary Table S1).

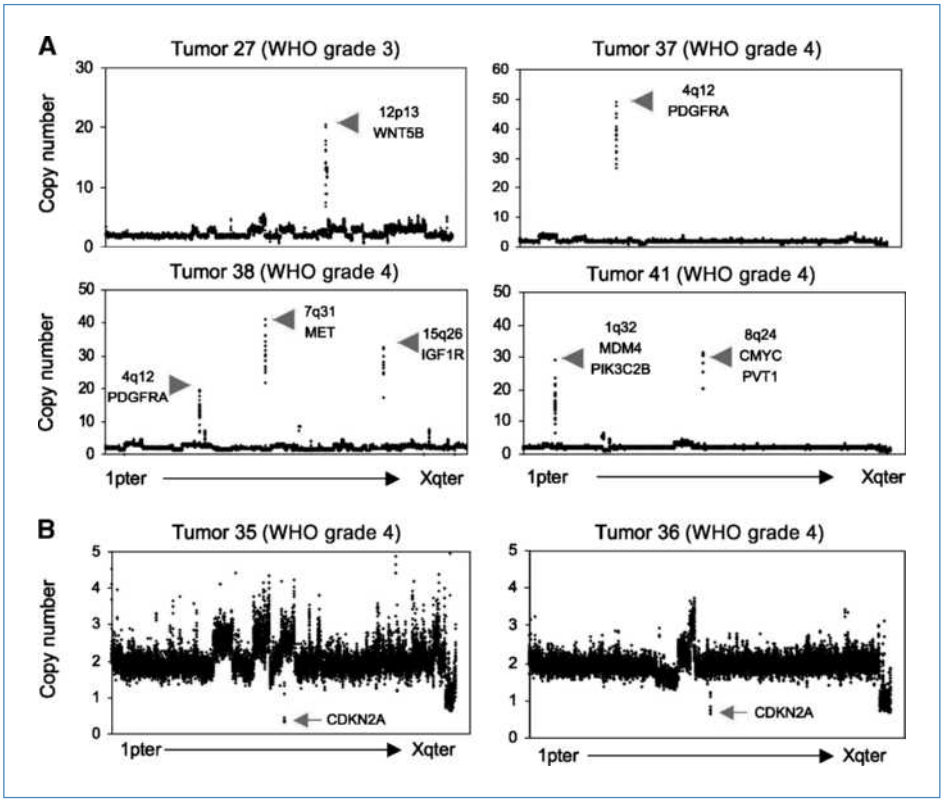

Figure 2. High-level amplifications and HDs in pediatric astrocytoma. Examples of genome copy number plots for tumors with high-level (>10 copies) genomic amplifications (*A*) and for tumors showing focal HDs of the *CDKN2A* locus (*B*).

Table 2. Recurrent gene alterations in pediatric astrocytomas

Gene alteration	No. occurrences	Tumor malignancy grade distribution
KIAA1549-BRAF: fusion	10	10 grade 1
BRAF: V600E	7	2 grade 2, 3 grade 3, and 2 grade 4
CDKN2A: HD	7	2 grade 2, 2 grade 3, and 3 grade 4
TP53: mutation or HD	6	2 grade 3 and 4 grade 4
PTEN: mutation or HD	2	2 grade 4
PDGFRA: amplification	2	2 grade 4

As revealed by the copy number aberration results (Fig. 1; Table 1), genomic alterations in grade 1 and 2 tumors are exceedingly rare. Nonetheless, a single recurrent alteration was identified in two grade 1 tumors and a single grade 2 tumor: a 2-Mb duplication at 7q34, with breakpoints encompassing the *KIAA1549* and *BRAF* genes (Fig. 3*A*). Duplications of this region have been associated with *KIAA1549-BRAF* rearrangements, resulting in the production of fusion mRNAs detectable by reverse transcription-PCR (RT-PCR; refs. 7–9). To determine whether the 7q34 duplications represented *KIAA1549-BRAF* fusion transcripts, mRNA was isolated from each of the initial cohort of 33 tumors and examined for these products. Both of the grade 1 tumors expressed *BRAF* fusion transcripts, but not the grade 2 tumor with a similar duplication of 7q34 (Fig. 3*B*). Eight additional grade 1 astrocytomas subsequently examined by RT-PCR all revealed expression of *KIAA1549-BRAF* fusion transcripts. In total, 10 of 10 PAs expressed one of the three common *KIAA1549-BRAF* fusion transcripts previously described (7), whereas none of 31 grade 2, 3, and 4 tumors expressed these fusion transcripts (Fig. 3*B*).

In addition to the gene rearrangements of *BRAF* resulting in the synthesis of *KIAA1549-BRAF* fusion transcripts, a missense activating *BRAF* mutation ($BRAF^{V600E}$) has been previously reported in grade 1 and 2 astrocytomas at low incidence (6, 7). Here, DNA sequence analysis revealed $BRAF^{V600E}$ mutation in 0 of 10 grade 1, 2 of 11 (18%) grade 2, 3 of 9 (33%) grade 3, and 2 of 11 (18%) grade 4 astrocytomas (Fig. 4*A*; Tables 1 and 2). MIP analysis indicated that both glioblastoma multiforme (GBM) tumors with $BRAF^{V600E}$ had 7q34 copy number gains (Fig. 4*B*), consistent with the relative peak areas of the *BRAF* DNA sequence tracings seen in these tumors (Fig. 4*A*). *BRAF* copy number gains were not evident in the three grade 3 tumors or two grade 2 tumors with $BRAF^{V600E}$ mutations.

Genes that are frequent mutagenic targets in the development of adult astrocytoma include *TP53, PTEN*, and *IDH1* (4, 5, 12). To address the incidence of these alterations in pediatric astrocytomas, we sequenced relevant coding regions of each of these genes in the current set of tumors. Sequence alterations of *TP53* were identified in five cases (two grade 3 and three grade 4 tumors), *PTEN* in one case (one grade 4 tumor), and *IDH1* in none of the tumors (Table 1). Activating mutation of *KRAS*, an infrequent occurrence in both adult and pediatric astrocytoma, was found in one grade 4 astrocytoma lacking the $BRAF^{V600E}$ alteration (Table 1). Together, these data show that *BRAF* is the most common mutagenic target in pediatric astrocytomas (Table 2). Specifically, 17 of 41 tumors had *BRAF* alterations followed by *CDKN2A* HD (7 instances) and *TP53* sequence alteration or HD (6 instances). Inactivating mutation and/or deletion of *PTEN* and amplification of *PDGFRA* were the only other specific gene alterations observed in multiple tumors (two tumors each).

We next examined gene alterations that occur concomitant with *BRAF* mutation and found that *CDKN2A* HD was observed in five of the seven tumors with the $BRAF^{V600E}$ alteration (Table 1). Among grade 2 to 4 tumors, the association between *CDKN2A* HD and $BRAF^{V600E}$ mutation was significant: Whereas 71% of grade 2 to 4 tumors with $BRAF^{V600E}$ have *CDKN2A* HD (5 of 7), only 8% (2 of 24) of the remaining grade 2 to 4 astrocytomas lacking the $BRAF^{V600E}$ mutation harbored *CDKN2A* HD ($P = 0.0016$, two-sided Fisher's exact test). In fact, no additional specific gene alterations, including those resulting from high-level genomic amplifications, were evident in the two remaining grade 3 tumors with $BRAF^{V600E}$ mutation (Table 1).

Because increased MAPK signaling accompanies BRAF activation, we next examined pMAPK expression in astrocytomas (14, 15). Interestingly, all pediatric astrocytomas examined (40 cases), irrespective of malignancy grade or *BRAF* mutation status, showed strong immunoreactivity for pMAPK (Supplementary Fig. S1).

Discussion

Grade 2 to 4 pediatric astrocytomas share histopathologic similarities with their corresponding adult counterparts, and, in general, pathologic examination does not distinguish pediatric and adult tumors of the same malignancy grade. Numerous studies have identified signature genetic mutations in high-grade adult astrocytomas, including the recent TCGA analysis of GBM tumors (4). The TCGA study showed that *EGFR, PTEN*, and *TP53* changes are among the most frequently observed alterations in adult GBM, whereas recent studies using parallel genomic approaches showed that mutations in the *IDH1* gene predominate in adult gliomas (5, 16). With the possible exception of *TP53* mutation, the frequent genetic alterations seen in adult astrocytomas have been identified at lower frequencies in pediatric astrocytomas (2, 3, 17). This lack of signature genetic mutations in pediatric astrocytomas is unfortunate, as these serve as important reference points with which to test therapeutic hypotheses.

The results of the current study further emphasize the distinct genetic etiologies of pediatric and adult astrocytomas. In our series, the only common adult astrocytoma gene alterations observed at appreciable frequencies were *CDKN2A* HD (7 of 31 cases, 23%) and alterations affecting p53 function (6 of 31 cases, 19%). The incidence of these alterations, however, is much lower than that reported by the TCGA project for adult GBM (4). Although a negative observation, the lack of *IDH1* mutation in the current series of astrocytomas is further evidence of the distinct genetic nature of the pediatric tumors. In this regard, a recent study that included 42 pediatric gliomas examined for *IDH1* mutation also concluded that these alterations are rare in childhood astrocytomas (18).

The approach taken here to identify common alterations in pediatric astrocytoma involved microarray analysis for high-resolution whole-genome examination. The SNP platform used has particularly high-density coverage of 1,000 genes associated with human cancer, yet has sufficient coverage for identifying focal gains and deletions across the majority of the genome (median distance between probes, across the entire genome, is 43 kb), and certainly has sufficient density to identify copy number alterations affecting all large chromosomal regions. Whereas recurrent copy number alterations indicating low-level gains or hemizygous deletions are of importance, and are presented in Supplementary Table S2, it is the regions of high-level amplification and HD that are of particular interest in revealing specific oncogene and tumor suppressor gene targets, respectively (Tables 1 and 2; Supplementary Table S1). These array data highlight *PDGFRA* and *CDKN2A* as important oncogene and tumor suppressor gene targets, respectively, in the development of pediatric malignant astrocytoma.

The identification of focal 7q34 copy number gains with rearrangement in three tumors (Fig. 3*A*) prompted an analysis of *BRAF* alterations, revealing *KIAA1549-BRAF* fusion transcript expression in 10 grade 1 tumors but not in a single grade 2 tumor with this genomic alteration. Although it is possible that there are additional *KIAA1549-BRAF* alterations not detected with the primer pairs we used, it seems that *BRAF* fusion transcripts are highly diagnostic of pediatric grade 1 astrocytoma. This is particularly important in clinical practice, as biopsy material from these tumors arising in the brainstem or optic nerve may not be representative of the entire tumor, and PA may be misdiagnosed as grade 2 or 4 astrocytoma. The development of reagents for immunohistochemical detection of the junction sequences in paraffin-embedded tissues would therefore be of great value.

In light of prior reports indicating a few instances of $BRAF^{V600E}$ activating mutations in grade 1 and 2 pediatric

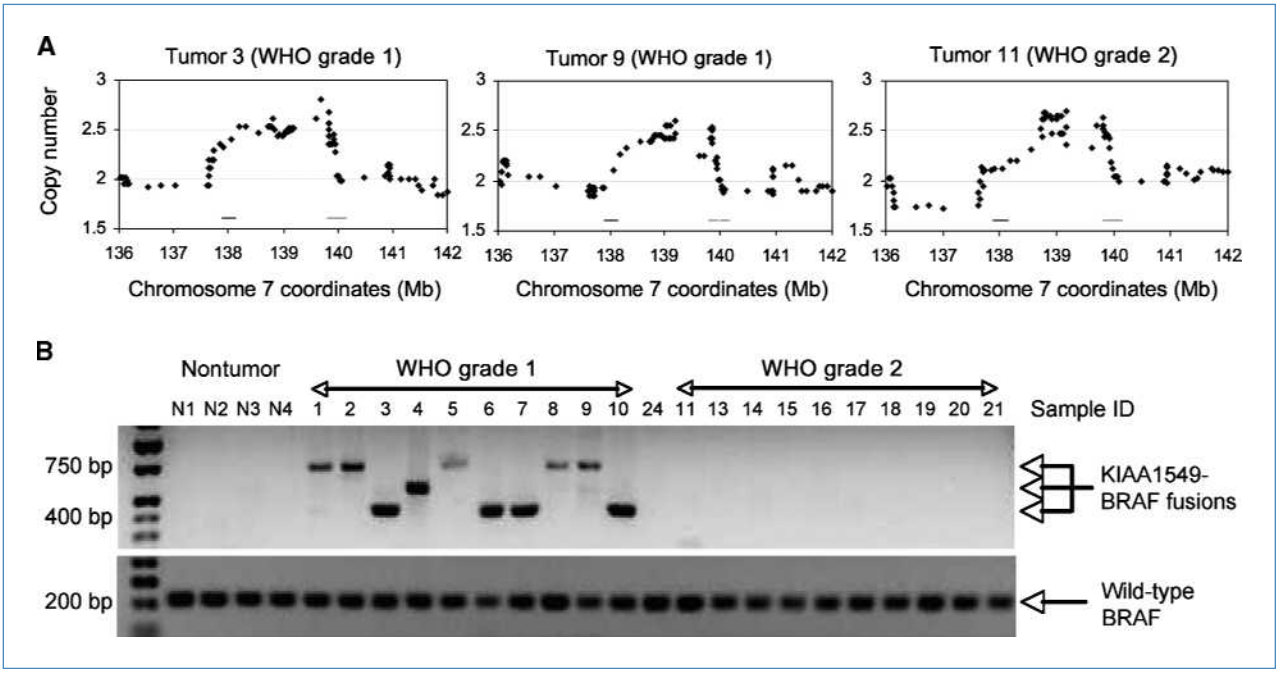

Figure 3. *BRAF* fusion alterations are common in PA tumors. *A,* high-resolution view of copy number duplications at 7q34 and juxtaposition of *BRAF* (*left horizontal line* at position 138) and *KIAA1549* (*right horizontal line* at position 140) sequences in grade 1 and 2 tumors. *B,* RT-PCR analysis of *KIAA1549-BRAF* fusion transcripts in nonneoplastic brain (*N1–N4*), grade 1 astrocytoma (n = 10), grade 2 astrocytoma (n = 10), and one grade 3 astrocytoma (tumor 24) reveals selective expression of fusion transcripts in grade 1 tumors. RT-PCR analysis of wild-type *BRAF* serves as a positive control. DNA sequencing of the RT-PCR fusion products revealed expression of *KIAA1549*-exon-15/*BRAF*-exon-9 transcripts (highest mobility fragment: four cases), *KIAA1549*-exon-16/*BRAF*-exon-11 transcripts (intermediate fragment: one case), and *KIAA1549*-exon-16/*BRAF*-exon-9 transcripts (lowest mobility fragment: five cases). Note that one grade 2 astrocytoma displayed a 7q34 duplication (tumor 11), but no *KIAA1549-BRAF* fusion transcript was detected.

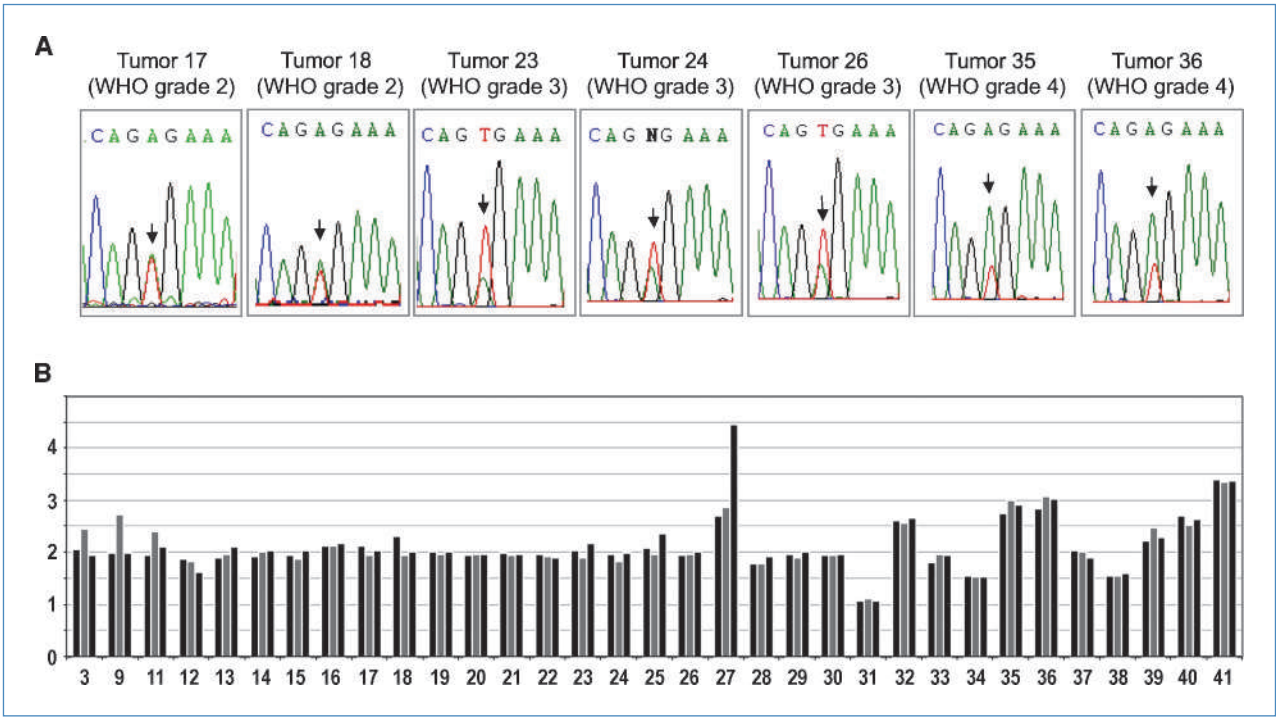

Figure 4. *BRAF* mutation in pediatric astrocytomas. *A,* sequence traces from grade 2, 3, and 4 astrocytomas showing the presence of both BRAF wild-type alleles (*T*) and mutant (*A*) $BRAF^{V600E}$ alleles in all instances where the V600E mutation has occurred. *B,* average copy number variation across 7q34. For each tumor, copy number was calculated for a ~2-Mb region inclusive of *KIAA1549* and *BRAF* (*gray columns*), a 5-Mb region proximal to *KIAA1549* and *BRAF* (*left black columns*), and a 5-Mb region distal to *KIAA1549* and *BRAF* (*right black columns*). This data representation highlights tumors with duplications limited to *KIAA1549* and *BRAF* (tumors 3, 9, and 11) and tumors with duplications of a larger 7q34 chromosomal region that includes *KIAA1549* and *BRAF* (tumors 32, 35, 36, 39, 40, and 41). Tumor 27 contains a 7q34 duplication and further 7q34 amplification distal to *BRAF*.

astrocytomas (6, 7), we determined the presence or absence of this alteration in the current series of tumors to address the overall incidence of *BRAF* alterations. Unexpectedly, seven tumors with $BRAF^{V600E}$ mutation were identified among the 31 grade 2 to 4 tumors (23%), suggesting that this alteration is one of the most common gene alterations in pediatric malignant astrocytomas (Table 2). Observation of *KRAS* activating mutation (Table 1), high-level *PDGFRA* or *MET* amplification (Table 1), and low-level copy number increases of *PTK2* (Supplementary Table S2) in seven additional grade 3 and 4 tumors that lack $BRAF^{V600E}$ indicates the occurrence of *BRAF* or surrogate genetic alterations for achieving heightened *BRAF* activity in most, and perhaps all (as implied by Supplementary Fig. S1 results), pediatric astrocytomas.

Even more surprising than the number of instances of $BRAF^{V600E}$ in pediatric grade 2 to 4 astrocytomas was the occurrence of *CDKN2A* HD in five of the seven tumors with $BRAF^{V600E}$: a frequency of co-occurrence that is highly significant. This association is underscored by the lack of other specific gene alterations occurring in combination with $BRAF^{V600E}$. $BRAF^{V600E}$ in combination with *CDKN2A* inactivation has been described in other cancers, especially melanoma (19), and in a recent report, this combination was identified in 2 of 18 grade 2 pediatric astrocytomas (8). Our results reinforce the importance of coincident $BRAF^{V600E}$ with *CDKN2A* HD in pediatric malignant astrocytomas and suggest that this combination of gene alterations occurs at similar frequencies across grade 2 to 4 tumors.

Finally, there are several BRAF signaling pathway inhibitors currently in clinical trial (20), including inhibitors of MAPK, a key downstream effector of BRAF. Interestingly, our immunohistochemical results indicate that MAPK activity is not differentially elevated in tumors with *BRAF* alterations (Supplementary Fig. S1), and suggest that additional activators of MAPK may be deregulated in pediatric astrocytoma. Studies are under way to determine how BRAF controls astrocyte cell growth as well as to assess the effect of MAPK inhibitors on deregulated BRAF-mediated astrocytoma growth. Moreover, the new pediatric astrocytoma–associated genetic mutations identified in this report should inform the development of more relevant animal models of pediatric astrocytoma.

Disclosure of Potential Conflicts of Interest

No potential conflicts of interest were disclosed.

Acknowledgments

We thank Cynthia Cowdrey for her outstanding assistance in tissue acquisition and processing.

Grant Support

Pediatric Low Grade Astrocytoma Foundation (J.G. Hodgson, D.H. Rowitch, and C.D. James), National Brain Tumor Society (D.H. Gutmann), Pediatric Brain Tumor Foundation (J.G. Hodgson, S.R. VandenBerg, D.H. Rowitch, M.S. Berger, and C.D. James), Harriet H. Samuelsson Foundation (J.D. Schiffman), Center for Children's Brain Tumors at Lucile Packard Children's Hospital (J.D. Schiffman, P.G. Fisher, J.M. Ford, and H. Ji), and NIH grants CA097257 (M.S. Berger and C.D. James), CA101777 (J.G. Hodgson), CA121940, and HG000205 (P. Flaherty). D.H. Rowitch is a Howard Hughes Medical Institute Investigator.

The costs of publication of this article were defrayed in part by the payment of page charges. This article must therefore be hereby marked *advertisement* in accordance with 18 U.S.C. Section 1734 solely to indicate this fact.

Received 5/22/09; revised 10/17/09; accepted 11/5/09; published OnlineFirst 1/12/10.

References

1. van't Veer LJ, Bernards R. Enabling personalized cancer medicine through analysis of gene-expression patterns. Nature 2008;452:564–70.
2. Raffel C, Frederick L, O'Fallon JR, et al. Analysis of oncogene and tumor suppressor gene alterations in pediatric malignant astrocytomas reveals reduced survival for patients with PTEN mutations. Clin Cancer Res 1999;5:4085–90.
3. Pollack IF, Hamilton RL, James CD, et al. Rarity of PTEN deletions and EGFR amplification in malignant gliomas of childhood: results from the Children's Cancer Group 945 cohort. J Neurosurg 2006; 105:418–24.
4. The Cancer Genome Atlas Network. Comprehensive genomic characterization defines human glioblastoma genes and core pathways. Nature 2008;455:1061–8.
5. Parsons DW, Jones S, Zhang X, et al. An integrated genomic analysis of human glioblastoma multiforme. Science 2008;321:1807–12.
6. Pfister S, Janzarik WG, Remke M, et al. BRAF gene duplication constitutes a mechanism of MAPK pathway activation in low-grade astrocytomas. J Clin Invest 2008;118:1739–49.
7. Jones DT, Kocialkowski S, Liu L, Pearson DM, Ichimura K, Collins VP. Tandem duplication producing a novel oncogenic BRAF fusion gene defines the majority of pilocytic astrocytomas. Cancer Res 2008;68:8673–7.
8. Forshew T, Tatevossian RG, Lawson AR, et al. Activation of the ERK/MAPK pathway: a signature genetic defect in posterior fossa pilocytic astrocytomas. J Pathol 2009;218:172–81.
9. Yu J, Deshmukh H, Gutmann RJ, et al. Alterations of BRAF and HIPK2 loci predominate in sporadic pilocytic astrocytoma. Neurology 2009;73:1526–31.
10. Wang Y, Moorhead M, Karlin-Neumann G, et al. Allele quantification using molecular inversion probes (MIP). Nucleic Acids Res 2005;33:e183.
11. Wang Y, Moorhead M, Karlin-Neumann G, et al. Analysis of molecular inversion probe performance for allele copy number determination. Genome Biol 2007;8:R246.
12. Balss J, Meyer J, Mueller W, Korshunov A, Hartmann C, von Deimling A. Analysis of the IDH1 codon 132 mutation in brain tumors. Acta Neuropathol 2008;116:597–602.
13. Lièvre A, Bachet JB, Boige V, et al. KRAS mutations as an independent prognostic factor in patients with advanced colorectal cancer treated with cetuximab. J Clin Oncol 2008;26:374–9.
14. Bar EE, Lin A, Tihan T, Burger PC, Eberhart CG. Frequent gains at chromosome 7q34 involving BRAF in pilocytic astrocytoma. J Neuropathol Exp Neurol 2008;67:878–87.
15. Sievert AJ, Jackson EM, Gai X, et al. Duplication of 7q34 in pediatric low-grade astrocytomas detected by high-density single-nucleotide polymorphism-based genotype arrays results in a novel BRAF fusion gene. Brain Pathol 2009;19:449–58.
16. Yan H, Parsons DW, Jin G, et al. IDH1 and IDH2 mutations in gliomas. N Engl J Med 2009;360:765–73.
17. Pollack IF, Finkelstein SD, Burnham J, et al. Age and TP53 mutation frequency in childhood malignant gliomas: results in a multi-institutional cohort. Cancer Res 2001;61:7404–7.
18. Hartmann C, Meyer J, Balss J, et al. Type and frequency of IDH1 and IDH2 mutations are related to astrocytic and oligodendroglial differentiation and age: a study of 1,010 diffuse gliomas. Acta Neuropathol 2009;118:469–74.
19. Haluska FG, Tsao H, Wu H, Haluska FS, Lazar A, Goel V. Genetic alterations in signaling pathways in melanoma. Clin Cancer Res 2006;12:2301–7s.
20. Montagut C, Settleman J. Targeting the RAF-MEK-ERK pathway in cancer therapy. Cancer Lett 2009;283:125–34.